# Micellization Behavior of $(PS)_8(PI)_8$ Miktoarm (Vergina) Star Copolymers

**S. Pispas, Y. Poulos, and N. Hadjichristidis***

*Department of Chemistry, University of Athens, Panepistimiopolis, Zografou, 157 71 Athens, Greece*

*Received March 9, 1998; Revised Manuscript Received April 30, 1998*

ABSTRACT: The static and hydrodynamic properties of micelles formed by $(PS)_8(PI)_8$ 16-miktoarm (Vergina) star copolymers in the selective, for the PI arms, solvent *n*-decane were studied. Static and dynamic light scattering and viscometry were employed to determine the aggregation number, the size, and shape of the micelles in dilute solutions. All samples formed multimolecular micelles in *n*-decane. For the low molecular weight symmetric sample, experiments indicate that the micelles have a more elongated shape. As the compositional asymmetry increased in favor of the soluble branches, the micelles become more spherical. In comparison to linear diblocks with block lengths equal to the lengths of the respective branches, miktoarm stars order into micelles of lower aggregation number and larger dimensions. The area, on the core−corona interface, per junction point was found to be larger in the miktoarm stars. The differences can be attributed to the differences in architecture and the additional constraints imposed by a common junction point in these highly branched miktoarm stars, which influence the organization of the macromolecules into stable micellar structures in solution.

## Introduction

Block copolymers dissolved in a selective solvent, i.e., a solvent good for one of the blocks but a precipitant for the other, tend to form supramolecular assemblies, the micelles.[1] The phenomenon was observed many years ago and since then has been investigated in considerable detail. Most of the studies were concerned with the micellization of linear diblock copolymers, the simplest possible architecture for a block copolymer.[2−8]

More complex well-defined architectures and especially miktoarm star copolymers have only recently attracted the interest of scientists working in this field, due to the advances in the synthesis of such materials.[9−14] From the results so far it is obvious that macromolecular architecture has emerged as an important parameter for manipulating molecular properties in conjunction with the chemical nature and chemical composition of the copolymers, molecular weight, solvent quality, concentration, and temperature in solution. Thus, one has the ability to control the final properties of the system and further design new molecules that may produce new entities in solution with different properties for particular applications.[8]

In this paper, we report on the solution properties of micelles formed by three well-defined 16-miktoarm star copolymers of the type $(PS)_8(PI)_8$ (Vergina stars), where PS is polystyrene and PI is polyisoprene, in *n*-decane, a selective solvent for the PI branches. We use static and dynamic light scattering and viscometry to investigate the influence of the common junction point from which two groups of eight arms, different in chemical nature, radiate on fundamental properties of the micelles such as aggregation number, size, and shape. Since these miktoarms can be considered to be produced from the connection of eight diblock copolymer chains attached to each other by the middle junction point, we compare our findings with results from diblocks having the same chemical constitution and block lengths as the PS and PI branches of the Vergina stars.

**Table 1. Molecular Characteristics of 16-miktoarm (Vergina) Star Copolymers Determined in Common Good Solvents**

| | VS1 | VS2 | VS3 |
|---|---|---|---|
| $M_w \times 10^{-5}$ [a] | 3.30 | 7.10 | 8.94 |
| $M_w$ PS arm $\times 10^{-4}$ [a] | 2.09 | 4.36 | 4.36 |
| $M_w$ PI arm $\times 10^{-4}$ [a] | 2.02 | 4.82 | 7.12 |
| $M_w/M_n$ [b] | 1.07 | 1.05 | 1.05 |
| wt % PS [c] | 48 | 49 | 41 |
| $[\eta]$ (mL/g) [d] | 48.3 | 72.4 | 111.9 |
| $R_v$ (nm) [d] | 13.6 | 20.1 | 25.1 |
| $k_H$ [d] | 0.89 | 0.88 | 0.72 |
| $D$ (cm$^2$/s) $\times 10^7$ [e] | 3.19 | 2.36 | 1.90 |
| $R_h$ (nm) [e] | 14.8 | 20.0 | 24.8 |
| $k_D$ [e] | 47 | 68 | 118 |

[a] By LALLS in THF at 25 °C. [b] By SEC. [c] By $^1$H NMR. [d] In toluene at 35 °C. [e] In THF at 25 °C.

## Experimental Section

**Polymer Synthesis.** All samples were synthesized by anionic polymerization high-vacuum techniques. The appropriate amount of living PSLi was reacted with a chlorosilane dendrimer having 16 active Si−Cl bonds in order to produce an 8-arm star. At the end of this coupling reaction a sample was withdrawn and fractionated. The molecular characterization, by low-angle laser light scattering (LALLS), has shown that the reactive intermediate possessed eight polystyrene arms. The remaining chlorosilane bonds were reacted with excess PILi arms of the desired molecular weight. The fractionated final products (pure miktoarm stars) were rigorously characterized by size exclusion chromatography/UV, membrane osmometry, LALLS, and NMR in order to provide the molecular characteristics of the materials. These measurements confirmed the high degree of compositional, molecular weight, and architectural homogeneity of the copolymers. Details on the synthesis and the molecular characterization of the miktoarm stars were given elsewhere.[15] The molecular characteristics of the samples under study are given in Table 1. Samples VS1 and VS2 have the same overall composition, but the molecular weights of each kind of arm in VS1 are half the molecular weights of the arms in VS2. Sample VS3 has the lower PS content, but its PS arms have the same molecular weight as the PS arms in VS2. Thus we

S0024-9297(98)00361-1 CCC: $15.00 
Published on Web 06/13/1998

can extract information about the micellar behavior of Vergina stars as a function of composition and molecular weights of each branch.

**Solvent Purification and Solution Preparation.** Analytical grade *n*-decane was dried over $CaH_2$ by refluxing for 24 h and was fractionally distilled. Stock solutions were prepared by dissolving a weighted amount of sample in the appropriate volume of dried solvent. Heating of the stock solutions at 60 °C overnight was necessary for complete dissolution of the samples. The most difficult to dissolve was sample VS2 with the higher PS arm molecular weight and PS content where VS3 was relatively the easiest to be dissolved. Heating at 60 °C with occasional stirring was continued for a further 2 h after the complete dissolution of the material to ensure absence of nonequilibrium structures related to memory effects from the solid-phase morphology of the samples. Solutions were weighted after heating, and the appropriate concentration corrections were made in order to account for loss of solvent. Stock solutions had the characteristic bluish tint related to the presence of micelles of considerable size in solution. No polymer precipitation was observed from these solutions after standing at room temperature for weeks. Solutions of lower concentration were obtained by subsequent dilution of the stock solutions. Before light-scattering measurements the solutions were filtered through 0.45 $\mu$m nylon filters, whereas for viscosity measurements, 1.2 $\mu$m nylon filters were used.

**Methods.** Initial light-scattering measurements were performed at 25 °C with a Chromatix KMX-6 low-angle laser light-scattering photometer, equipped with a 2 mW He−Ne laser operating at $\lambda = 633$ nm. Apparent weight average molecular weights, $M_w$, and second virial coefficients, $A_2$, were obtained from the concentration dependence of the reduced scattering intensity. Multiangle light-scattering measurements were conducted with a Series 4700 Malvern system composed of a PCS5101 goniometer with a PCS7 stepper motor controller, a Cyonics variable power $Ar^+$ laser, operating at 488 nm and with 10 mW power, a PCS8 temperature control unit, and a RR98 pump/filtering unit. Apparent mean square radii of gyration, $R_g$, were determined by the initial slope of the angular dependence of the reduced scattering intensity. Dried over $CaH_2$ and fractionally distilled toluene was used as a calibration standard. The general equation for light scattering was used in this case

$$Kc/\Delta R_\theta = 1/M_w\{1 + [(16\pi^2 n_o^2)/(3\lambda_o^2)]\langle R_g^2\rangle \sin^2(\theta/2)\} + 2A_2c + ... \quad (1)$$

where $K = (2\pi n_o)^2(dn/dc)^2(N_A\lambda_o^4)^{-1}$, $c$ is the polymer concentration, $\Delta R_\theta$ is the excess Rayleigh ratio, $\theta$ is the scattering angle, $n_o$ is the solvent refractive index, $\lambda_o$ is the wavelength of light in a vacuum, $dn/dc$ is the specific refractive index increment, and $N_A$ is the Avogadro number.

Dynamic light-scattering experiments were carried out, at 25 °C, on the same Malvern system operating in the dynamic mode. A 192 channel correlator was used for accumulation of the data. Correlation functions were analyzed by the cumulant method and the Contin software provided with the instrument. The correlation function was collected at angles between 45 and 120°. There was no indication of the presence of unimers from Contin analysis at the concentration range studied for each sample. In this region the equilibrium is shifted in favor of the micelles and the properties measured correspond to the micelles. The ratio $\mu_2/\Gamma^2$, where $\mu_2$ is the second cumulant and $\Gamma^2$ the decay rate, derived from cumulant analysis was <0.1 for all angles and concentrations, indicating low polydispersity of the micelles. Apparent diffusion coefficients at zero concentration, $D_{o,app}$, were obtained after extrapolation to zero angle by the use of eq 2, where $D_{app}$ is

$$D_{app} = D_{o,app}(1 + k_D c) \quad (2)$$

the diffusion coefficient measured at each concentration and $k_D$ is the coefficient at the concentration dependence of $D_{app}$.

**Table 2. Results from Static Light Scattering on Micelles of the Vergina Star Copolymers in *n*-Decane at 25 °C[a]**

| sample | $M_{w,app} \times 10^{-6}$ | $A_2 \times 10^6$ | $R_g$ (nm) | $N_w$ |
|---|---|---|---|---|
| VS1 | 8.88 | 2.3 | 45.5 | 27 |
| VS2 | 81 | 1.2 | 42.5 | 114 |
| VS3 | 44 | 2.5 | 46.3 | 49 |

[a] We estimate a 10% error in the experimentally determined $M_w$ and a 15% error in $A_2$ and $R_g$.

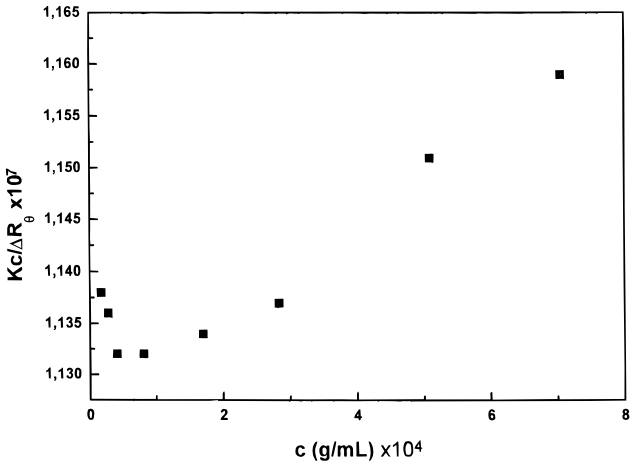


**Figure 1.** $Kc/\Delta R_\theta$ vs concentration plot for sample VS1 in *n*-decane at 25 °C.

Apparent hydrodynamic radii, $R_h$, were determined by

$$R_h = k_B T/6\pi\eta_o D_{o,app} \quad (3)$$

where $k_B$ is the Boltzmann constant, $T$ is the absolute temperature, and $\eta_o$ is the viscosity of the solvent.

For the viscosity measurements, Cannon-Ubbelohde dilution viscometers were used in a temperature controlled bath ($\Theta = 25 \pm 0.02$ °C). Flow times for the solvent and the micellar solutions were measured with a Scott-Gerate AVS 410 automatic flow timer. Data were analyzed by aid of the Huggins (4) and Kraemer (5) equations, where $[\eta]$ is the intrinsic

$$\eta_{sp}/c = [\eta] + k_H[\eta]^2 c + ... \quad (4)$$

$$\ln \eta_r/c = [\eta] + k_K[\eta]^2 c + ... \quad (5)$$

viscosity and $k_H$ and $k_K$ are the Huggins and Kraemer coefficients, respectively. Viscometric radii, $R_v$, were calculated from

$$R_v = (3/10\pi N_A)^{1/3}([\eta]M_{w,app})^{1/3} \quad (6)$$

where $M_{w,app}$ is the weight average molecular weight determined by light scattering.

## Results and Discussion

The results from static light-scattering experiments in *n*-decane are given in Table 2. A representative plot is given in Figure 1. For all samples, curves of $Kc/\Delta R_\theta$ vs $c$ were bent upward at low concentrations in all cases, as a consequence of the shift of the micellization equilibrium in favor of the micelles as the concentration increases. No indication of critical micelle concentration (cmc) was observed even at the lower concentrations studied, which means that the cmc must be very low for these systems and outside the experimentally accessible region. $M_w$, $A_2$, and $R_g$ values correspond to the linear part of the curve at higher concentrations where the properties measured are dominated from the

**Table 3. Results from Dynamic Light Scattering for the Vergina Star Micelles in *n*-Decane at 25 °C**

| sample | $D \times 10^8$ (cm²/s) | $k_D$ | $R_h$ (nm) |
|---|---|---|---|
| VS1 | 6.3 | 92 | 40.2 |
| VS2 | 3.2 | −130 | 79.0 |
| VS3 | 3.6 | 125 | 70.2 |

presence of micelles. Estimated molecular weights are elevated, in comparison to the molecular weights of the copolymers, indicating the formation of multimolecular micelles in this solvent. The $A_2$ values are very small as a result of the high molecular weight of the micelles and the poor thermodynamic environment. Due to the low $A_2$ values and the high d$n$/d$c$ values for both miktoarm star components in *n*-decane the $M_{w,app}$ values calculated from the linear part of the curves must be very close to the true molecular weight of the micelles. The weight average aggregation numbers defined as

$$N_w = M_{w,micelle}/M_{w,unimer}$$

increase as the molecular weight of the insoluble branches increase (VS1 vs VS2) and decreases as the PI arm length increases (PS content decreases, VS2 vs VS3). The same situation was observed in the linear diblock case.[5,6] Thus sample VS1 has the lower aggregation number and sample VS2 the highest. However the $R_g$ value for VS2 is the smallest, while VS1 and VS3 have similar $R_g$'s, something that is rather surprising and may be due to the different arrangement of the molecules in the micelles of the different samples. We will return to this point later.

The results from dynamic light scattering are given in Table 3. The diffusion coefficients are lower than the values in a good solvent due to the lower mobility of the supramolecular structures. $k_D$ values do not show a definite trend, maybe due to different results from the balance between hydrodynamic and thermodynamic interactions ($k_D = 2A_2M - k_f - v$), represented by this parameter, for each sample. The $R_h$ values seem to follow the trend in the variation of aggregation number. Thus, micelles of sample VS1 have the lower aggregation number and the smallest hydrodynamic radius where for sample VS2 the micelles have the largest aggregation number and the largest $R_h$. The experimental $D_{app}$ vs $c$ curves are given in Figure 2.

The viscometric results are given in Table 4. Here the intrinsic viscosities measured for the micellar solutions are smaller than the ones measured in a good solvent. This can be attributed to the collapse of the insoluble PS chains that form a core of small dimensions, and only the PI arms are well solvated. The $k_H$ values are large due to the increased hydrodynamic interactions within the micelles. The larger $k_H$ is observed for sample VS1, indicating that these micelles must be more compact than the ones formed from the other samples. Due to the high $k_H$ values, the slope of the Kraemer equation becomes positive, as observed in many associating systems. The $R_v$ value calculated from static light scattering and viscometry is smaller than $R_h$ in the case of VS1 where both radii have similar values for sample VS3. A representative plot is given in Figure 3.

To gain some insight for the shape of the micelles formed by the $(PS)_8(PI)_8$ miktoarm stars, the ratios $R_v/R_h$ and $R_g/R_h$ were calculated for each case. The results are shown in Table 5. The ratio $R_v/R_h$ increases from VS1 to VS3, i.e., as PS content decreases and PS

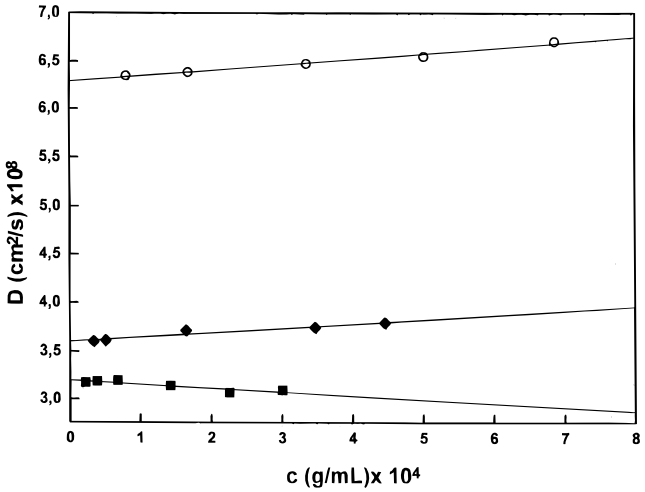


**Figure 2.** Concentration dependence of diffusion coefficient for samples VS1 (○), VS2 (■), and VS3 (◆) in *n*-decane at 25 °C.

**Table 4. Viscometric Results on the Vergina Star Micelles in *n*-Decane at 25 °C**

| sample | $[\eta]$ (mL/g) | $k_H$ | $R_v$ |
|---|---|---|---|
| VS1 | 19.6 | 1.09 | 30.2 |
| VS2 | 25.2 | 0.83 | 68.6 |
| VS3 | 39.7 | 0.89 | 64.9 |

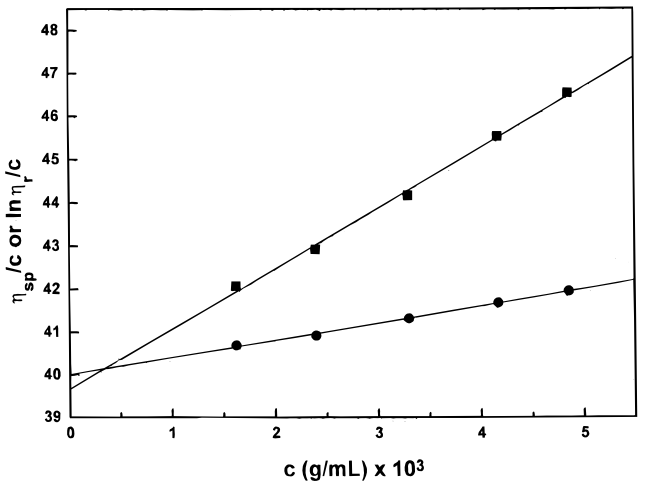


**Figure 3.** Huggins (■) and Kraemer (●) plots for sample VS3 in *n*-decane at 25 °C.

**Table 5. Values for the Ratios of the Different Radii for the Micelles Formed by the Vergina Star Copolymers**

| | sample or model | | | | | |
|---|---|---|---|---|---|---|
| | VS1 | VS2 | VS3 | hard spheres | spheres with soft surface | model of ref 17 |
| $R_v/R_h$ | 0.748 | 0.868 | 0.924 | 1.00 | | |
| $R_g/R_h$ | 1.13 | 0.538 | 0.660 | 0.775 | 0.70 | 0.60 |

molecular weight increases. The PI arm molecular weight increases in that order too. The behavior of the ratio $R_g/R_h$ is more complicated. $R_g/R_h$ is the largest for sample VS1 with 50/50 composition and the lower molecular weights of the arms. Upon comparison of samples VS2 and VS3, $R_g/R_h$ increases as the molecular weight of the soluble arms increases. The ratios $R_v/R_h$ and $R_g/R_h$ are equal to 1 and 0.775 for hard homogeneous spheres, respectively.[16] A value of $R_g/R_h > 1.0$ usually corresponds to more elongated structures.[7] Additionally, the $R_g/R_h$ ratio is a measure of the radial density distribution of a particle in solution.[7,17] For a

sphere of radius $R = R_h$ having a soft surface, $R_g/R_h = 0.70$, while a triangular radial distribution yields $R_g/R_h = 0.63$.[18] The radial density distribution model considered in ref 17, which better represents the density distribution in a micelle with a collapsed core and solvated corona, gives $R_g/R_h = 0.60$.

The value $R_g/R_h = 1.13$ for sample VS1 may indicate that the micelles formed by these macromolecules have a more elongated shape in an attempt to release chain crowding around the central junction point, which in this case must be located on the interface separating the insoluble PS arms from the solvated PI chains in the corona. For the PI chains it is difficult to be located at the surface of a sphere, so the assembly grows in one dimension in order to find some additional space for the swelled chains.

Looking at the situation from the view of geometrical packing of a miktoarm molecule in space, with the junction point located on a curved surface, we come to the same conclusions. Sample VS3 has a large soluble part and a small insoluble part (considering the contraction of the PS arms in the bad solvent environment). This leads to a cone morphology for the single star molecule and to a relatively high curvature for the core−corona interface in the micelle. Sample VS1, with a smaller difference in the relative sizes of the soluble and insoluble parts, can form a more or less truncated cone. The resulting curvature is smaller in this case and the micelles can become more elongated.

These elongated structures may be rather loose and they can be disrupted under the shear forces developed in the capillary tube, resulting in more stable aggregates giving lower viscosities and lower $R_v/R_h$ ratios, as observed in several associating systems.[7,19] The shape of VS3 micelles seems to be closer to a sphere as $R_v/R_h$ is closer to unity and the $R_g/R_h$ value is closer to a sphere with a "soft" outer surface. The case of VS2 micelles seems to be a more complicated one. $R_v/R_h$ approaches unity, indicating approach to hard sphere behavior. However, the $R_g/R_h$ value is lower than the one expected for spheres. Similar low values for the ratio $R_g/R_h$ have also been observed, by Schmidt et al., in solutions of microgels.[17] They proposed a radial density distribution model for their case with a rather smooth decrease of density across the radius of the dissolved species, which we believe describes well the density distribution in a miktoarm micelle. Thus the shape of micelles formed by the Vergina stars depends on the relative lengths of the different arms, providing a means of manipulating nanostructures in solution.

At this point a comparison of the micellar properties of the Vergina stars with their corresponding linear diblocks with the same block lengths as the arms of the miktoarms or the same total molecular weight and composition is in order. Bahadur et al.[5] studied a PS−PI diblock having $M_{w,PI} = 20\,000$ and $M_{w,PS} = 19\,000$, which are very close to the molecular weights of the arms of sample VS1. They report an aggregation number of 386 chains per micelle in *n*-heptane, a hydrocarbon with a selectivity toward PI similar to that of *n*-decane, and $R_h = 27.5$ nm in *n*-decane. The aggregation number of VS1 is 1 order of magnitude lower than the one for the linear diblock. Even after multiplication of the experimental $N_w$ for VS1 by 8 (the number of constitutive diblocks for these miktoarm stars), we end up with 216 diblock chains per micelle, still less than the observed $N_w$ for the diblock. The $R_h$ for the linear diblock is close to the $R_v$ for VS1 but is lower than $R_h$ of the Vergina star, something that can be attributed to differences in the micellar shape. It seems that, in the case of miktoarm micelles with no external perturbation, the dimensions are larger, although the number of blocks in the core and the corona of the micelles are lower. The difference may be solely due to the elongated shape of the VS1 micelles.

In another investigation, Oranli et al.[6] studied a series of PS−PBd diblocks in aliphatic solvents, selective for PBd, a system similar to our case. A sample of total $M_n = 375\,000$ and 48 wt % PS in heptane, which is close to the total molecular weight and composition of VS1, formed micelles with an aggregation number of 233 molecules/micelle. This is again almost 1 order of magnitude larger than the one determined for VS1. It seems that the particular $(PS)_8(PI)_8$ architecture is able to form stable micelles with lower aggregation numbers. This may be a result of better saturation of the core−corona interface by fewer corona chains. Due to localization of the junction point at this interface, the volume available to each arm is less than the simple diblock case. This results in a larger curvature of the interface.

One of Oranli's samples with $M_n = 46\,000$ and a PS content of 51 wt % in *n*-decane (analogous to VS1 constituting diblock) showed $N_w = 193$, which corresponds well with the number of constitutive diblock chains of the VS1 micelles (i.e., $N_w$ of VS1 multiplied by 8). In this case $R_h$ was equal to 28.2 nm, which that corresponds well with $R_v$ for VS1 but is smaller than $R_h$ of VS1. The remarks made before for the PS−PI diblock sample apply also here.

Another PS−PBd sample with $M_n = 72\,000$ and 52 wt % PS (corresponding to the constitutive diblock of VS2) formed micelles of 330 chains in heptane, which is much larger than the 114 molecules per micelle for sample VS2 but lower than 912, the number of constitutive diblocks in the VS2 micelles. $R_h$ for the diblock was 31 nm, whereas for the Vergina star $R_h$ is more than twice this value. In this last pair, the micellar shape is more or less spherical in both cases and again a larger stretching of the coronal chains in the miktoarm case must be the reason for the larger dimensions of the micelles formed by the Vergina star copolymers. It has to be mentioned that low aggregation numbers, in respect to the constitutive diblocks, were also observed in micelles formed by other types of $A_nB_n$ miktoarm stars.[12,13] Additionally, the concept of comparing aggregation numbers of miktoarms and constitutive diblock micelles may be a crude way of quantifying the different factors, including architecture, that play a decisive role in the formation of micelles in copolymers of complex architecture.

It is also interesting to compare the area of the core−corona interface per copolymer molecule in the case of simple diblocks and the 16-miktoarm stars. The area, A, per copolymer chain is given by

$$A = 4\pi R_c^2/N_w \tag{7}$$

where $R_c$ is the radius of the core, which in the case of a spherical PS core can be estimated by

$$R_c = (3M_{w\ mic}wt_{PS}/4\pi N_A d_{PS}\phi_{PS})^{1/3} \tag{8}$$

where $wt_{PS}$ is the weight fraction of the core-forming block, $d$ is the density of PS ($d = 1.06$ g/mL), and $\phi_{PS}$ is

**Table 6. Calculated Core Radii and Areas per Copolymer Chain for the Case of a Dry PS Core in Diblock and Vergina Star Spherical Micelles**

| sample | $M_{n,copol} \times 10^{-4}$ | wt % PS | $R_c$ (nm) | $A$ ($nm^2$) | area per constitutive diblock |
|---|---|---|---|---|---|
| SA-3[a] | 2.9 | 31 | 9.4 | 4.5 | |
| SA-4[a] | 3.6 | 45 | 12.0 | 6.5 | |
| SA-5[a] | 3.9 | 49 | 14.0 | 6.4 | |
| SA-6[a] | 4.9 | 59 | 19.3 | 7.0 | |
| SA-7[a] | 5.3 | 62 | 23.9 | 6.4 | |
| VS2 | 71.0[b] | 49 | 24.6 | 66.7 | 8.3 |
| VS3 | 89.4[b] | 41 | 18.8 | 90.6 | 11.3 |

[a] From ref 5. [b] $M_w$ from light scattering (see Table 1).

the volume fraction of PS in the core, which depends on the swelling of the core by the solvent. For $\phi_{PS} = 1$ the core is completely dry, a situation not far from reality in the case of polystyrene in decane or heptane. In Table 6 the calculated values for $R_c$ and $A$ for the case of a dry PS core are given for the diblock PS−PI samples studied by Bahadur and co-workers[5] in heptane and for VS2 and VS3, which form micelles with a spherical shape. It can be concluded that the area per copolymer chain (or the area per junction point) is almost constant in the case of diblocks whereas for the Vergina stars it increases by increasing the length of the soluble block. Additionally, the area per junction point is larger for the case of the Vergina star micelles. Even if the area per junction is divided by the number of the constitutive diblocks of the 16-miktoarm stars, we still get an increased area per diblock chain in comparison with the diblock samples. A similar observation was made for the area per junction point of lamellae forming diblocks and Vergina stars in the bulk-ordered state.[20] This again can be attributed to the crowding of the arms in the 16-miktoarm stars due to the existence of one common juction point.

## Conclusions

The micelles formed by three 16-miktoarm (Vergina) star copolymers of the type $(PS)_8(PI)_8$ show a lower aggregation number than the corresponding constitutive diblocks or diblocks of similar total molecular weights and composition. A transition from elongated micelles at low molecular weight of the arms and symmetric composition to more spherical micelles at higher molecular weight and asymmetric composition is indicated through examination of the values for the ratios $R_v/R_h$ and $R_g/R_h$. For spherical micelles the area per copolymer chain was found to be larger in the case of the Vergina stars in comparison to simple diblocks. The results can be explained if one takes into account the topological constrains inherent to these molecules because of the presence of one central junction point for the chemically different arms. Intermolecular segregation of the PS blocks increases the crowding of the PI arms on one side of the core−corona interface. A compromise between screening the unfavorable PS−decane interactions and finding the required volume for the solvated coronal PI chains may result in altering the curvature of the interface together with an energetically preferred one-dimensional growth of the aggregate, which may lead to a change in the overall shape of the micelles.

## References and Notes

(1) Tuzar, Z.; Kratochvil, P. *Surf. Colloid Sci.* **1993**, *15*, 1.
(2) Tsunashima, Y.; Hirata, M.; Kawamata, Y. *Macromolecules* **1990**, *23*, 1089.
(3) Tsunashima, Y. *Macromolecules* **1990**, *23*, 2963.
(4) Stejskal, J.; Hlavata, D.; Sikora, A.; Konak, C.; Plestil, J.; Kratochvil, P. *Polymer* **1992**, *33*, 3675.
(5) Bahadur, P.; Sastry, N. V.; Marti, S.; Riess, G. *Colloids Surf.* **1985**, *16*, 337.
(6) Oranli, L.; Bahadur, P.; Riess, G. *Can. J. Chem.* **1985**, *63*, 2691.
(7) (a) Antonietti, M.; Heinz, S.; Schmidt, M.; Rosenauer, C. *Macromolecules* **1994**, *27*, 3276. (b) Calderara, F.; Riess, G. *Macromol. Chem. Phys.* **1996**, *197*, 2115.
(8) Antonietti, M.; Forster, S.; Oestreich, S. *Macromol. Symp.* **1997**, *121*, 75.
(9) Prochaska, K.; Glocker, G.; Hoff, M.; Tuzar, Z. *Makromol. Chem.* **1984**, *185*, 1187.
(10) Iatrou, H.; Willner, L.; Hadjichristidis, N.; Halperin, A.; Richter, D. *Macromolecules* **1996**, *29*, 581.
(11) Pispas, S.; Hadjichristidis, N.; Mays, J. W. *Macromolecules* **1996**, *29*, 7378.
(12) Tsitsilianis, C.; Papanagopoulos, D.; Lutz, P. *Polymer* **1995**, *36*, 3745.
(13) Tsitsilianis, C.; Kouli, O. *Macromol. Rapid Commun.* **1995**, *16*, 591.
(14) Ramzi, A.; Prager, M.; Richter, D.; Efstratiadis, V.; Hadjichristidis, N.; Young, R. N.; Allgaier, J. B. *Macromolecules* **1997**, *30*, 7171.
(15) Avgeropoulos, A.; Poulos, Y.; Hadjichristidis, N.; Roovers, J. *Macromolecules* **1996**, *29*, 6076.
(16) Yamakawa, H. *Modern Theory of Polymer Solutions*; Harper and Row: New York, 1971.
(17) Schmidt, M.; Nerger, D.; Buchard, W. *Polymer* **1979**, *20*, 582.
(18) Antonietti, M.; Bremser, N.; Schmidt, M. *Macromolecules* **1990**, *23*, 3796.
(19) Pispas, S.; Allorio, S.; Hadjichristidis, N.; Mays, J. W. *Macromolecules* **1996**, *29*, 2903.
(20) Beyer, F. L.; Gido, S. P.; Poulos, Y.; Avgeropoulos, A.; Hadjichristidis, N. *Macromolecules* **1997**, *30*, 2373.

MA980361N